IEEE/CSC & ESAS SUPERCONDUCTIVITY NEWS FORUM (global edition), November 2019.
Plenary presentation Wed-Mo-PL4-06 given at MT26, September 22 – September 27, 2019; Vancouver, Canada.

Development of a Nb_3Sn Superconducting Undulator for the Advanced Photon Source

I. Kesgin, M. Kasa, S. MacDonald, Y. Ivanyushenkov, Y. Shiroyanagi, Q. Hasse, E. Barzi, D. Turrioni, A.V. Zlobin, and E. Gluskin

***Abstract*—NbTi superconducting undulators (SCUs) are currently reliably operating at the Advanced Photon Source (APS) at Argonne National Laboratory (ANL). These devices have significantly enhanced x-ray flux and brightness at the high energy spectrum. As NbTi SCU technology is close to its full potential, further performance enhancement requires using different superconducting materials. Nb_3Sn is a promising candidate to achieve that goal. Recently the APS has started developing an Nb_3Sn double undulator compatible with the APS storage ring. The magnetic length of each Nb_3Sn undulator is about 1.4 m, totaling to 2.8 m. The completed device is planned to be installed in the APS storage ring. To develop the Nb_3Sn SCU technology, a series of short SCU models has been fabricated and successfully tested. The SCU magnet design is being scaled up to an intermediate length of ~0.5 m. In the course of the short model magnet R&D, performance and quench analysis of the design have been experimentally evaluated and improved and the details are presented.**

***Index Terms*—Nb_3Sn, superconducting undulator, SCU, stability, magnet design, quench.**

I. Introduction

THE ADVANCED PHOTON SOURCE (APS) has initiated a project that aims to build a ~2.8 m-long niobium-tin superconducting undulator (SCU) device that is planned to be installed into the APS's storage ring (SR). This device will be the world's first Nb_3Sn based SCU that will serve in routine user operations. Due to the challenge involved with the technology, the project is broken down into 3 phases. In the first phase, the design of the magnet has been progressively matured by fabricating and testing several short prototypes. One of the big challenges with the Nb_3Sn technology is that since the undulator operates in relatively lower on-conductor magnetic fields, the regular strands developed for high field magnets are not stable [1-3], and strands with smaller effective filament diameters are required. The strand requirements and optimizations for this project have been addressed in [2, 4] along with the heat treatment optimizations [5]. The required performance has also been confirmed in the first phase of the project along with the insulation and quench detection issues.

Manuscript received October 22, 2019. This work was supported by the U.S. Department of Energy, Office of Science, under Contract DE-ACO2-O6CH11357. (Corresponding author: Ibrahim Kesgin)

I. Kesgin, M. Kasa, S. MacDonald, Y. Ivanyushenkov, Y. Shiroyanagi, Q. Hasse, and E. Gluskin are with Advanced Photon Source, Argonne National Laboratory, Lemont, IL 60439 USA (e-mail: ikesgin@anl.gov).

E. Barzi, D. Turrioni, and A. V. Zlobin are with Fermilab, Batavia, IL 60510 USA.

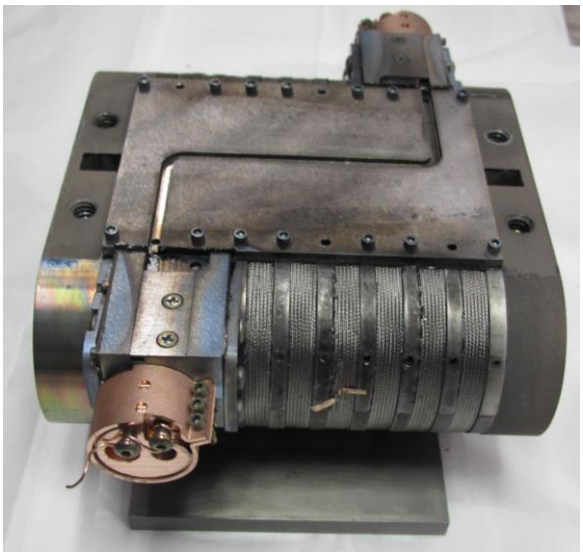

Fig 1. A picture of short model magnet 6 (SMM6) after winding and reaction before the epoxy impregnation.

The second phase of the project focuses on the scalability of the short model design, quality of the generated on-axis magnetic field, and further analysis of quench behavior. These findings will further mature the design that will allow scaling the model to 1.4-m-long storage ring compatible magnets in the last phase. In parallel to Nb_3Sn magnet developments, the cryostat and its subcomponents along with storage ring vacuum system interfaces are being developed.

Currently, phase one of the project has been completed and details are presented in the following sections. The model is also being scaled up to an intermediate (~0.5 m) -length model magnet, and this is now being tested. The cryostat main components, namely, vacuum vessel, thermal shield, and helium tank, are also currently being fabricated.

II. Nb_3Sn Superconducting Undulator Design

A. Magnet design

The magnetic and mechanical designs of the short Nb_3Sn model magnets (SMMs) were completed and several prototypes were fabricated and tested. These were reported in an earlier publication [4]. The expected performance has been confirmed; however, this first design was not compatible with

TABLE I
SHORT MODEL MAGNET (SMM) DESIGN PARAMETERS

Design parameters	SMM3	SMM4 and SMM5	SMM6
Number of periods	4.5	4.5	4.5
Groove width (mm)	5.4	5.3	5.5
Groove depth (mm)	5.5	4.7	4.9
Period length (mm)	18	18	18
Turns in each groove (46)	46	46	46
Conductor	RRP 150/169	RRP 150/169	RRP 144/169
Conductor diameter (mm)	0.6	0.6	0.6
Insulation thickness (μm)	65	65	65

the cryostat design and also indicated some weak mechanical behavior [4]. To address these issues and incorporate the lessons-learned from these model magnets, the design was further modified. The magnet was reduced in height and stretched in width slightly to fit in the cryostat. The design parameters for the short model magnets (SMMs) are provided in Table I. The magnets were wound in a similar fashion to their NbTi counterparts and reacted using a similar heat treatment cycle that was developed at Fermilab during the first model magnet design [4]. After the heat treatments, the magnets were vacuum pressure impregnated (VPI) and tested in a liquid helium bath. A picture of the fabricated SMM after winding and reaction is provided in Fig 1.

As SMM4 showed some weak insulation behavior, thin mica layer was inserted between the Nb_3Sn wire and the winding core in SMM6 and an extra insulation layer was added in locations where Nb_3Sn wire transitions from one groove to another. SMM6 was successfully tested and provided enough confidence on the maturity of the design. Then, the SMM6 design was scaled-up to intermediate length of 0.5 m without any modifications.

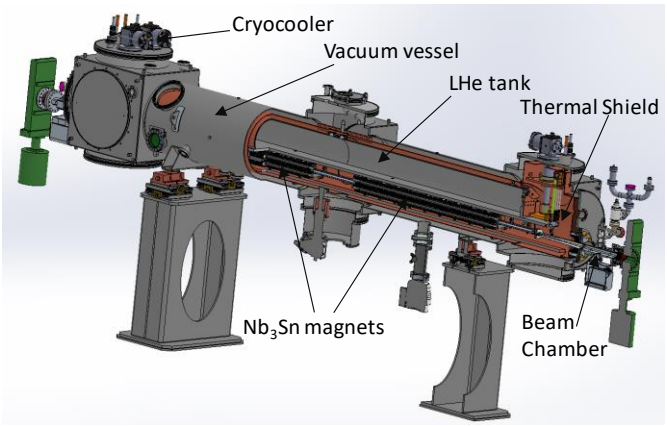

Fig 2. Nb_3Sn SCU cryostat 3D model with major components. Cutout section shows vacuum vessel, LHe tank, thermal shield, beam chamber and Nb_3Sn magnets. It has 5 cryocoolers cooling the shield and a low-temperature circuit that runs about 4.2 K. A dedicated cryocooler cools the beam vacuum chamber.

B. *Cryostat*

A new 4.8-meter-long cryostat is being fabricated for the Nb_3Sn SCU. This cryostat will house two 1.4-m-long double Nb_3Sn magnet pairs. This cryostat is capable of housing more than 4-m-long undulator magnetic structure. Thermal analysis of the cryostat has been performed and a number of required cryocoolers have been chosen. Fig 2 shows the overall cryostat design with five cryocoolers. The design is flexible, using mostly off-the-shelf components and will allow addition of extra cryocoolers if needed. This cryostat is basically an extension of the helical SCU cryostat that was built and is now operating at the APS [6, 7]. Fig 2 shows a general view of the major cryostat components, including the vacuum vessel, the thermal shield, and the liquid helium reservoir. Five cryocoolers cool the thermal shield (runs about 45 K) and a low temperature thermal circuit that runs about 4.2 K. A dedicated cryocooler for cooling the beam vacuum chamber is also located at the center bottom turret.

The magnets are cooled by liquid helium in the center channels that runs along the magnet's length. The liquid helium flows through these channels via the thermosiphon effect.

III. RESULTS AND DISCUSSIONS

A. *RRR*

RRR is an important parameter for the hot spot temperature and also influences the stability of the conductor. A higher RRR is required, but typically it comes at the expense of reduced performance. The RRR of SMM6 is about 52. The short-sample RRR measurement, 54, agree well with the magnet measurements that is an indication of well-controlled, uniform reaction process.

B. *Training*

The training results for SMM3-6 are summarized in Fig 3a. All prototypes reached the maximum design operating current of 875A (straight black line) except SMM4. SMM3, 5 and 6 were tested successfully, and no degradations in their performances were observed after many quenches at well above the maximum design current. SMM4 failed after reaching the maximum design current. SMM6 fabrication capitalized on the experience accumulated and lessons learned in the process of building/winding and testing all its previous prototypes. Particularly important lessons were learned from SMM4. It resulted in degradation after it reached the design current, and therefore specific design changes were implemented in SMM5 and SMM6 to prevent such shorts. The reason for failure was identified to be multiple shorts to the core. These design changes eliminated the shorts, and the magnet reached noticeably higher current levels than the designed operating current. SMM3 and SMM5 performed very similarly and hardly required any training to reach the max operating current – one or two quenches at most. Short sample limits are also provided in the same figure for each SMM.

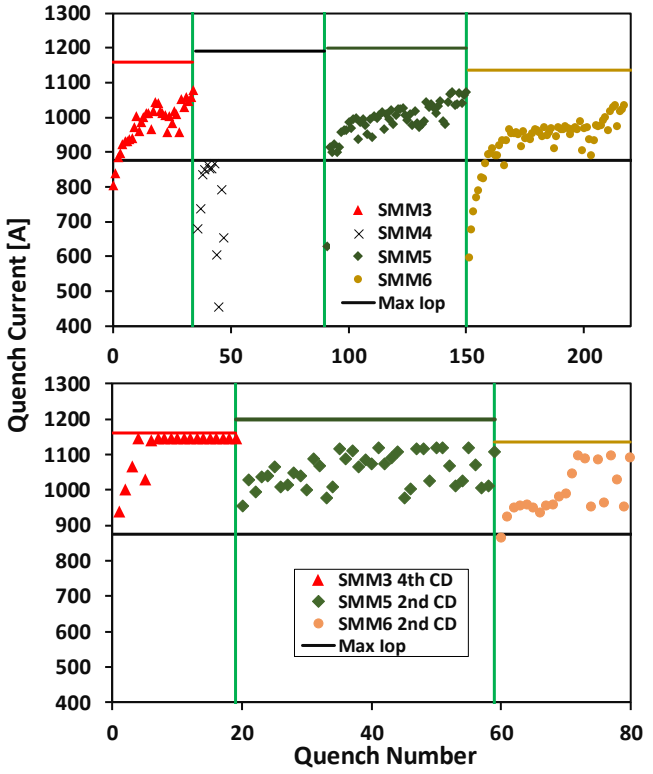

Fig 3. Training curves for SMM3-6 in the first cool down (a) and after the repeated cool down(s) (b) except SMM4 which was damaged in the first CD. Magnets reached the maximum operating current and required a few quenches. The second CD showed that the magnet has very good memory and requires almost no training to reach the maximum operating current.

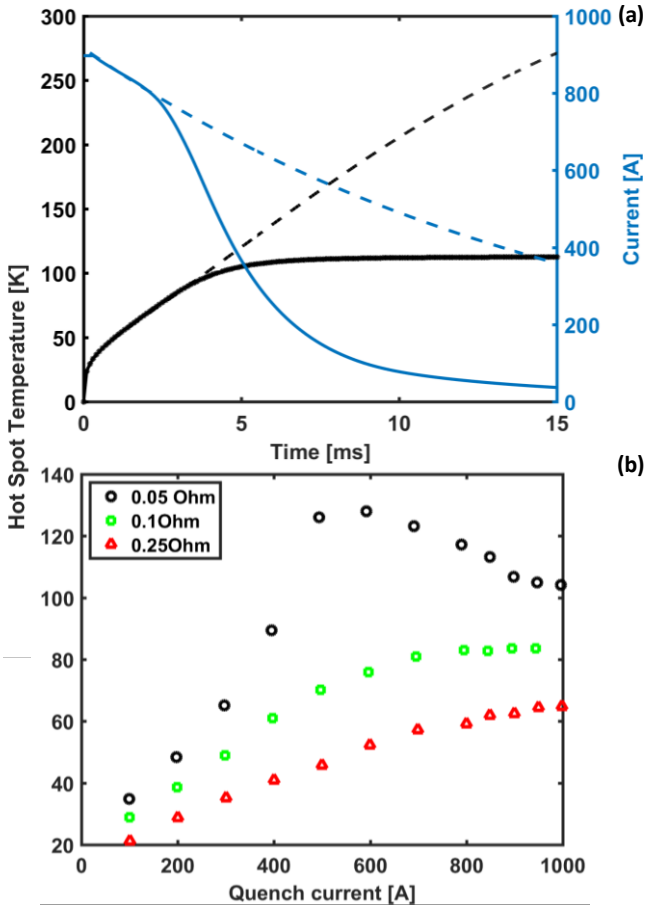

Fig 4. Hot spot temperatures versus time (a) and current (b). Dynamic losses contribute to the resistance growth inside the magnet and the current decays faster. This behavior is more pronounced at higher currents and reduces the hot spot temperature as shown in (b). The effect becomes less when the resistance increases.

The model magnets' results after cool down (CD) cycles are summarized in Fig 3b. SMM3 reached about 100% of its short sample limit (SSL) after several CD cycles. SMM5 reached 93% and SMM6 has reached 96% of their SSLs after two thermal cycles. After the thermal cycles, the models required almost no training to reach the operating current, indicating a good training memory.

C. Quench analysis

In the event of a quench, the current flowing in the superconductor is transferred to the copper around the superconducting filaments making the copper current density very high and if the stored energy in the magnet is not safely removed, detrimental consequences can occur. An active protection scheme was implemented with an external dump resistor to protect Nb3Sn magnets and Lawrence Berkeley National Laboratory develops a dedicated system to protect the Nb_3Sn undulator in the SR. Experimental studies with the last short model magnet (SMM6) were conducted to identify the upper limits on the quench parameters. The three major parameters that define the limits for safe operation of a superconducting magnet are: hotspot temperature formed during a quench, terminal voltage or coil to ground voltage, and resistive voltage grown inside the Nb_3Sn winding. The maximum voltage the magnet can withstand was experimentally found to be 500 V (break-down voltage), and we are improving this number by introducing a mica insulation layer between the Nb_3Sn strands and the metal core. The maximum hotspot temperature of 300 K is considered safe.

During a quench, a hot spot forms and the hot spot temperature can be calculated, assuming an adiabatic system, by integrating the I^2 over the time span and using the temperature dependent material properties. The hotspot temperatures are calculated by this method is very conservative, and the real temperature is lower than the calculated ones.

Current decay profiles in the case of a 50 mΩ dump resistor are provided in Fig 4a. The model magnets showed strong dynamic loss contribution, which causes significant internal resistance growth. This behavior is evident from Fig 4a as the current decay is faster about 3 ms after the quench is initiated. Such an effect significantly reduces the hot spot temperature. In the same figure, a pure exponential current decay profile is represented by dashed lines and the resultant hot spot temperature is calculated, which approaches the safe limit of 300 K even at about a 60% current decay. Although these calculations are conservative, this number is close to the temperature limit of 300K. It is important to note that these quenches are artificial, meaning that the current is kept at a certain value

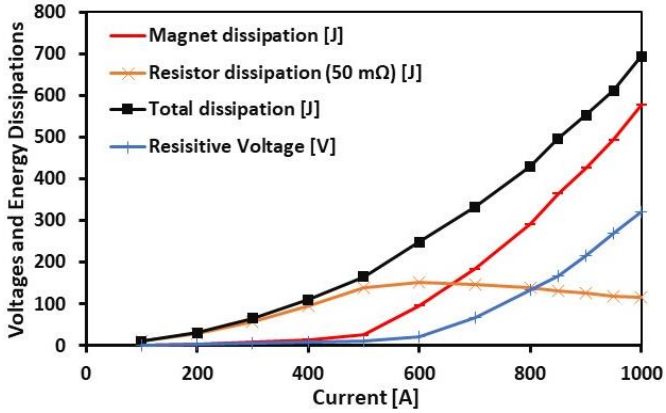

Fig 5. Resistive voltage and dissipated energies versus artificially induced quench current. Resistive voltage is not noticeable until 500A and it starts growing after 500 A. Consequently, a portion of the stored energy dissipates into the magnet, and energy dissipations into the dump resistor decrease.

and quench detection is manually triggered. The real quench is triggered by a voltage drop caused by a hot spot formed due to a small disturbance that exceeds the minimum quench energy. The relevant voltage drop activates the detection system.

In Fig 4b, the calculated hot spot temperatures are shown with respect to quench currents with different dump resistors. Due to the faster current decays at higher current values, the hot spot temperatures are either reduced or kept the same. This effect becomes less noticeable when the resistor value is increased. As expected, the hot spot temperatures are also reduced by increasing resistor values.

D. Voltage and Energy Dissipations during Quench

After a quench is detected, the power supply is separated from the circuit and an LR circuit is formed. Then the quench parameters are calculated as described in [4].

Fig 5 shows various parameters and their changes with current. The value of the dump resistor used for these tests were 50 mΩ. The maximum resistive voltage formed due to the growth of the non-superconducting portion inside the magnet during a quench is negligible up to 500A and is very close to zero. In conjunction with that behavior, the energy dissipated into the magnet is very low up to 500A; it grows rapidly beyond that current level. That means most of the stored energy is deposited to the magnet at higher currents, whereas the dump resistor takes most of the stored energy at current levels smaller than 500 A. The energy dissipated into the dump resistor is at its maximum around 500 A and decreases when the current increases. The total dissipated energy is also provided in Fig 5 and these values reasonably agree with the calculated values from the $(½)LI^2$. The dynamic loss contribution is very helpful in reducing the hot spot temperature at higher currents. From these results, it is clear that the protection of the undulator magnets seems to be more challenging at intermediate current levels. These analyses need to be experimentally confirmed for longer magnets. Therefore, in Phase II of the project, more rigorous quench analyses will be conducted.

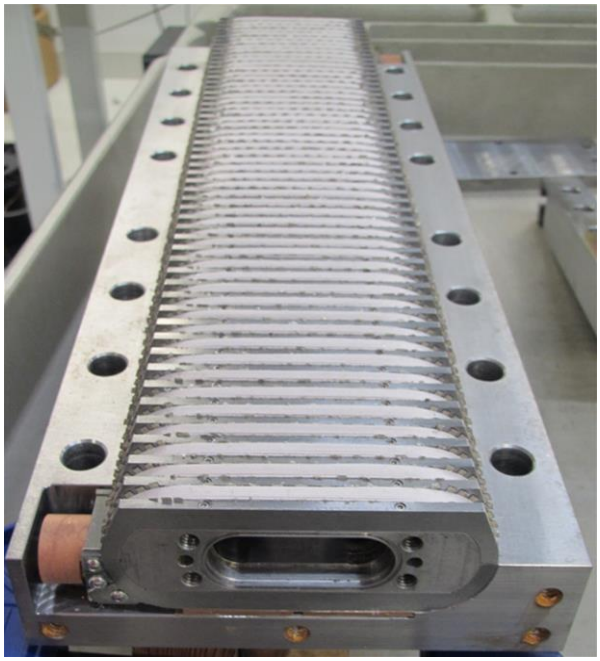

Fig 6. A picture of Nb_3Sn intermediate length (~0.5m-long) model magnet after winding inside the reaction tooling.

After the design delivered the expected performance level and it was proven that the magnets could be protected, the magnet was scaled to an intermediate length of 0.5 m. A picture of the wound magnet before the reaction is seen in Fig 6. The magnet is currently being epoxy impregnated and will be tested thereafter.

IV. Conclusion

The Advanced Photon Source has started developing a 4.8-m-long superconducting undulator cryostat consisting of two 1.4 m long double Nb_3Sn magnetic structures. The project has three phases and in Phase I, short Nb_3Sn model undulator magnets were successfully fabricated and tested. Step-by-step improvements of the magnet design and fabrication procedure were implemented and quench behavior was analyzed. After the expected performance confirmed and showed that the magnet can be safely protected, the design was scaled to intermediate length in Phase II that is currently ongoing. After completion of the Phase II, the magnetic structure will be scaled up to a 1.4 m long magnet in the final phase. In parallel, the cryostat and its subcomponents as well as the vacuum chamber and its storage ring interfaces will be completed. The final assembly will be characterized offline and confirmed that the APS storage ring specs are fulfilled, then it will be installed to the APS's SR for user operation, which will serve as the first Nb_3Sn SCU photon source operating in a light source.

References

[1] S. O. Prestemon *et al.*, "Design, fabrication, and test results of undulators using Nb_3Sn superconductor," *IEEE Transactions on Applied*

Superconductivity, vol. 15, no. 2, pp. 1236-1239, 2005, doi: 10.1109/TASC.2005.849540.

[2] A. V. Zlobin, E. Barzi, D. Turrinoni, Y. Ivanyushenkov, and I. Kesgin, *Advantage and Challenges of Nb3Sn Superconducting Undulators* (Conference: 9th International Particle Accelerator Conference, Vancouver, BC Canada, 04/29-05/04/2018). JACoW Publishing, 2018, p. Medium: ED.

[3] H. W. Weijers, K. R. Cantrell, A. V. Gavrilin, E. L. Marks, and J. R. Miller, "Assembly Procedures for a Nb_3Sn Undulator Demonstration Magnet," *IEEE Transactions on Applied Superconductivity*, vol. 17, no. 2, pp. 1239-1242, 2007, doi: 10.1109/TASC.2007.899988.

[4] I. Kesgin *et al.*, "Development of Short-Period Nb3Sn Superconducting Planar Undulators," *IEEE Transactions on Applied Superconductivity*, vol. 29, no. 5, pp. 1-4, 2019, doi: 10.1109/TASC.2019.2897645.

[5] E. Barzi, M. Kasa, I. Kesgin, D. Turrioni, and A. V. Zlobin, "Heat threatment studies of Nb_3Sn wire for supeconducting planar undulators," *IEEE Transactions on Applied Superconductivity*, vol. Submitted, 2020.

[6] J. Fuerst *et al.*, "Review of New Developments in Superconducting Undulator Technology at the APS," in *ICFA Advanced Beam Dynamics Workshop on Future Light Sources (FLS2018)*, Shanghai, China, March 5-9, 2018 2018: JACoW.

[7] M. Kasa *et al.*, "Design, Construction, and Magnetic Field Measurements of a Helical Superconducting Undulator for the Advanced Photon Source," in *9th International Particle Accelerator Conference (IPAC 2018)*, Vancouver, BC Canada, April 29-May 4, 2018.